Estuarine, Coastal and Shelf Science 310 (2024) 108988

Contents lists available at ScienceDirect

Estuarine, Coastal and Shelf Science

journal homepage: www.elsevier.com/locate/ecss

Association between water darkening and hypoxia in a Norwegian fjord

Martine Røysted Solås [a,b,*], Anne Gro Vea Salvanes [a,b], Dag L. Aksnes [a]

[a] Department of Biological Sciences, University of Bergen, 5006 Bergen, Norway
[b] Bjerknes Centre for Climate Research, 5007 Bergen, Norway

ARTICLE INFO

Keywords:
Coastal water darkening
Deoxygenation
Hypoxia
Light attenuation
CDOM
Fjords

ABSTRACT

Previous studies have shown that climate change makes Norwegian fjords prone to deoxygenation and water darkening (reduced light penetration) with ecological implications across the food web from phytoplankton to fish. While deoxygenation occurs in deep fjord basins due to reduced water renewal, water darkening has primarily been linked to increased loads of colored dissolved organic matter (CDOM) of terrestrial origin in rivers draining to the Baltic Sea, the North Sea and ultimately to the Norwegian Coastal Current and associated coastal waters. Here, we investigate the hypothesis that water darkening is also linked to deoxygenation of fjord basins. We measure the downwelling irradiance in a water column with hypoxic and anoxic water and compare it with a nearby, well-oxygenated water column. Our data show increased darkening in the hypoxic and anoxic layers, likely due to elevated concentrations of CDOM that is produced locally in these layers. We discuss the ecological implication of this result, which we believe is particularly relevant for the mesopelagic habitat.

1. Introduction

Previous studies have shown that climate change makes Norwegian coastal waters and fjords prone to deoxygenation (Aksnes et al., 2019; Darelius, 2020; Johnsen et al., 2024) and water darkening (Aksnes et al., 2009; Frigstad et al., 2023; Opdal et al., 2023). Although "coastal water darkening" was first reported for fjords, it now more generally refers to the 20th century trend of decreasing light penetration of visible light such as reported for the North Sea (Capuzzo et al., 2015; Dupont and Aksnes, 2013; Opdal et al., 2019), the Baltic Sea (Fleming-Lehtinen and Laamanen, 2012; Kahru et al., 2022; Sandén and Håkansson, 1996), as well as for the Norwegian Coastal Water (NCW) which embraces the entire coast of Norway (Opdal et al., 2023, 2024). Such water darkening is an important driver of upper water processes such as photosynthesis and primary productivity, while also having implications for deeper waters where organisms depending on vision, such as many mesopelagic fish, are distributed.

Coastal water darkening has primarily been associated with increased supplies of colored dissolved organic matter (CDOM) of terrestrial origin, but also wind-driven resuspension of sediments in shallow areas (Capuzzo et al., 2015; Wilson and Heath, 2019) and elevated pigment and organic matter concentrations following eutrophication events (Fleming-Lehtinen and Laamanen, 2012; Stigebrandt and Andersson, 2020). A long-term increase in the loads of CDOM of terrestrial origin (hereby referred to as t-CDOM) has been linked to increased vegetation in Scandinavia and Northern Europe that has been connected to increased warming, precipitation, and changes in land use (Larsen et al., 2011; Opdal et al., 2023, 2024). The t-CDOM is transported with freshwater ultimately draining to the NCW that is carried northward along the Norwegian coast with the Norwegian Coastal Current (NCC, Fig. 1A) (Opdal et al., 2023; Sætre, 2007). Parts of this t-CDOM is labile and can thus be degraded within weeks in freshwater or upon entering the coastal system (Erlandsson and Stigebrandt, 2006), but a significant proportion is also recalcitrant and cause elevated light attenuation far from the original freshwater source (Højerslev et al., 1996; Opdal et al., 2023; Stedmon and Markager, 2003). The t-CDOM content of the NCW absorbs light and therefore decreases the water column light penetration (Frigstad et al., 2013; Opdal et al., 2023). Due to its freshwater content, NCW is less dense and floats above the more saline and transparent oceanic water (Aksnes, 2015; Sætre, 2007). This means that the direct effect from t-CDOM on light penetration is restricted to the NCW-layer. Due to the shading, however, the water masses below and all the way to the bottom also become darker with increased t-CDOM of the NCW layer.

Besides the water darkening caused by t-CDOM, previous evidence also suggests an additional darkening effect in deep fjord basins where low concentrations of dissolved oxygen occur (Aksnes et al., 2009). Due to lack of *in situ* light measurements at large depths, however, the actual

* Corresponding author. Department of Biological Sciences, University of Bergen, 5006 Bergen, Norway.
E-mail address: martine.solas@uib.no (M.R. Solås).

https://doi.org/10.1016/j.ecss.2024.108988
Received 16 June 2024; Received in revised form 1 October 2024; Accepted 14 October 2024
Available online 16 October 2024

darkening associated with such deoxygenation has until now not been measured. In the present study, we have selected a fjord, Haugsværfjorden, that is sufficiently shallow so that *in situ* light could be measured in water masses that were hypoxic, anoxic as well as in the well-oxygenated upper layer. To quantify a darkening effect expected to be associated with hypoxic and anoxic water, we compare the light penetration in Haugsværfjorden basin with that in the upper well-oxygenated 125 m of the neighbor fjord, Masfjorden, which Haugsværfjorden branches off from (Fig. 1B).

2. Materials & methods

2.1. Study area

Fjords are long and narrow inlets separated from the outer coast by sills, which are topographical barriers. The water renewal of a fjord basin, i.e., the volume of the fjord that is situated below the sill depth, can be limited and this can generate oxygen loss in the fjord basin over time (Aure and Stigebrandt, 1989). Such oxygen loss occurs in periods when microbial oxygen consumption of the fjord basin exceeds the oxygen supplied from water renewals. Our study site, Masfjorden (Fig. 1), is separated from the outer fjord Fensfjorden by a 75 m deep sill. This relatively deep sill provides good water exchange and connection with the NCC (Aksnes et al., 1989) which ensure good oxygen conditions above the sill depth as well as in the upper part of the fjord basin that has a maximum depth of 494 m. Haugsværfjorden, with a maximum depth of 125 m, branches off from Masfjorden over a 25 m deep sill. This ensures good water exchange with Masfjorden and consequently good oxygen conditions above the sill depth. The fjord basin of Haugsværfjorden, however, is prone to hypoxia and anoxia at depths at which downwelling irradiance can be measured with commercially available light meters.

Our observations were made during four research cruises with R.V. Kristine Bonnevie in Masfjorden and Haugsværfjorden 2020–2022 (Fig. 1; Table S1).

2.2. CTD deployments

Depth profiles of dissolved oxygen, salinity, temperature, and chlorophyll fluorescence were collected from CTD deployments (Sea-Bird SBE 9). Conductivity and oxygen sensors were calibrated, while chlorophyll fluorescence is reported in relative units (Supplementary S2).

2.3. Light measurements

Downwelling irradiance was measured using two hyperspectral RAMSES TriOS ACC spectroradiometers: one deck sensor and one underwater sensor. The surface sensor was mounted at the top of the wheelhouse of the ship, while the sub-surface sensor was deployed close to solar noon (±ca. 3 h) from the sunny side of the ship (see further details in Supplementary S3). We estimated the light attenuation of downwelling irradiance at wavelength 500 nm from the observed light penetration, which was represented as a fraction of surface light, $f_z = E_z/E_0$. Here, E_z and E_0 are the simultaneously measured irradiances at depth z and at the surface (i.e., with the deck sensor) respectively. We chose 500 nm because this is representative for the wavelengths that penetrated deepest into the water column of the two fjords. We also note that this wavelength is close to the peak sensitivity of the visual pigments of mesopelagic fish (480–492 nm; Warrant and Locket, 2004; Turner et al., 2009), a prominent organism group residing in the mesopelagic zone of Norwegian fjords as well as in the global ocean (Giske et al., 1990; Gjøsæter and Kawaguchi, 1980; Irigoien et al., 2014).

Following the methodology of Aksnes et al. (2017), for each deployment of the spectroradiometer, we estimated depth-specific light attenuation coefficients (K_{500}) as the slope in the linear regressions of ln (f_z) versus z for 10 m intervals. E.g., K_{500} at depth 50 m was derived from the measurements taken in the depth interval from 45 m to 55 m. Only K_{500} values from ln(f_z) regressions with a $R^2 \geq 0.95$ were used.

During the cruise in August 2021, CDOM measurements were conducted in Haugsværfjorden on water samples collected using Niskin water collectors mounted on the CTD. The CDOM concentrations were characterized by the spectrophotometric light absorption at 500 nm of water filtered through 0.22 μm (Sterivex-GP filters, Millipore). For the spectrophotometric light absorption reading we used a spectrophotometer (UV/VIS Spectrometer Lambda 2, PerkinElmer) with a 10 cm quartz cuvette. All measurements were relative to a cuvette with Milli-Q water measured at the start of analysis. Below, these absorption measurements are referred to as $a(\text{CDOM})_{500}$. See further details in Supplementary S4.

2.4. Data analysis

Previous studies in Norwegian fjords and coastal water report that the variations in salinity, chlorophyll, and dissolved oxygen account for part of the variation in quantities considered to be proxies for light attenuation (Aksnes, 2015; Opdal et al., 2023). These previous studies have used salinity as a proxy for t-CDOM, i.e., decreasing salinity (more freshwater influenced) means higher t-CDOM content.

In the present study, we examine to what extent the variation in the three water mass properties account for the attenuation coefficient, K_{500}, that we derived from actual measurements of downwelling irradiance (see section 2.3). We used a multiple regression analysis with K_{500} as the dependent variable and salinity, relative chlorophyll fluorescence, and dissolved oxygen as independent variables. Prior to the regression, we excluded 31 out of 277 datapoints in Haugsværfjorden and 15 out of 204 datapoints in Masfjorden because of NA values from the fluorometer.

All illustrations and analyses were done in R (R Core Team, 2022)

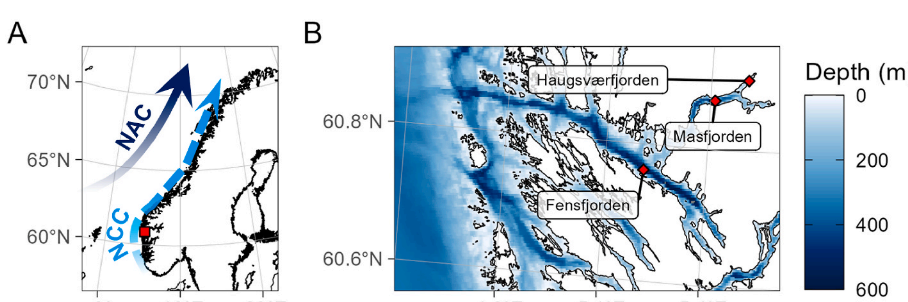

Fig. 1. Map of (**A**) Norway and location of study (red square) with simplified arrows illustrating the North Atlantic current (NAC) and Norwegian coastal current (NCC) and (**B**) the fjord system used in our study. Details about sampling can be found in Table S1. Norway land shape files are from the European Environment Agency (European Environment Agency, 2017; eea.europa.eu) and bathymetry data are from GEBCO (GEBCO Compilation Group, 2023; download.gebco.net). (For interpretation of the references to color in this figure legend, the reader is referred to the Web version of this article.)

with the additional packages tidyverse (Wickham et al., 2019), ggOceanMaps (Wihtakari, 2024), and lm.beta (Behrendt, 2022). For both the spectroradiometer and the CTD, depth was derived from measured pressure according to 1 dbar = 1 m seawater.

3. Results

Light penetrated deeper in Masfjorden than in Haugsværfjorden, with more than 10 times as much light penetrating to 100 m depth in Masfjorden compared to Haugsværfjorden (Fig. 2). This difference was due to an increase in light attenuation (K_{500}) at depths below ca. 50 m, i.e., in the hypoxic and anoxic layers of Haugsværfjorden (Fig. 3A and B). In contrast, K_{500} remained constant (or decreased slightly, Fig. 3A) below 50 m in the well-oxygenated Masfjorden (≈200 μmol O_2 kg^{-1}, Fig. 3B).

The difference in light penetration between the two fjords was lowest in June 2020 (Fig. 2). This was due to a prominent Deep Chlorophyll Maximum (DCM) around 40 m depth in Masfjorden as shown by the high relative chlorophyll fluorescence values (Fig. 3D) and the associated increase in K_{500} (Fig. 3A). The shading from this DCM caused a tenfold darkening at the depths below but was not sufficient to make Masfjorden darker than Haugsværfjorden at 100 m depth (Fig. 2). The largest difference in the light penetration between the two fjords was seen in March 2020 when a DCM was not present. At this time, the deepest light measurement in Haugsværfjorden (at 90 m depth) was ca. 14% of that measured at the same depth in Masfjorden (Fig. 2).

The association between water darkening and hypoxia was quantified using multiple regression analysis. The estimated standardized regression coefficients (β-values in Table 1) suggest that the variation in dissolved oxygen concentration accounted for a larger fraction of the variation in K_{500} than salinity and relative chlorophyll fluorescence did. Salinity and fluorescence are common proxies used for t-CDOM (lower salinity, more t-CDOM) and chlorophyll respectively. When removing water that were mildly hypoxic to anoxic from the regression analysis (i.e., only including measurements with dissolved oxygen >100 μmol kg^{-1}, n = 341), the effect of dissolved oxygen disappeared as a predictor of K_{500} (coefficient = −0.0000068, p-value > 0.1, β-value = −0.01). The absolute value of the salinity coefficient decreased somewhat (coefficient = −0.0172, p-value ≪ 0.001, β-value = −0.46) while chlorophyll fluorescence maintained a similar coefficient to the one in Table 1 (coefficient = 0.0276, p-value ≪ 0.001, β-value = 0.61), and the regression had an overall better fit to the data ($R^2_{adj.}$ = 0.83, p-value ≪ 0.001).

Our $a(\text{CDOM})_{500}$ measurements in Haugsværfjorden showed elevated CDOM concentrations in surface waters (Fig. S5). This is expected from the concurrent decrease in salinity towards the surface

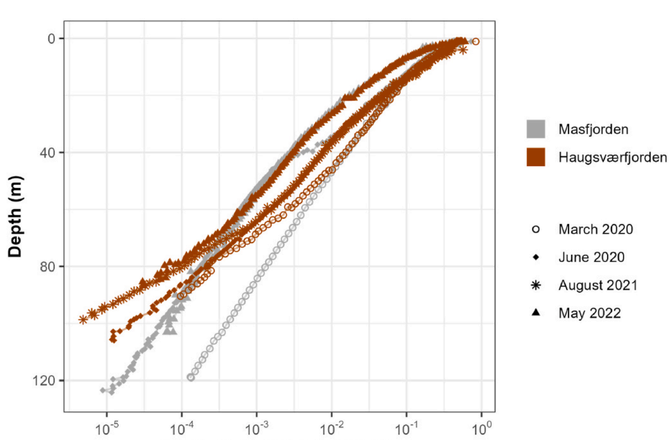

Fig. 2. Depth profiles (0–125 m) of light penetration at 500 nm (dimensionless, given as fraction of surface light; f_z) in Haugsværfjorden and Masfjorden. Sampling dates are listed in Table S1.

(Fig. 3C) showing increased influence of freshwater and its content of t-CDOM. The increases in $a(\text{CDOM})_{500}$, however, was even more pronounced (3- to 4-fold) when moving deeper into the hypoxic and anoxic layers, which are more saline and less influenced by freshwater than the layers above.

4. Discussion

Our results are consistent with the hypothesis that deoxygenation of fjords involve water darkening. This darkening comes in addition to the darkening associated with increased supplies of t-CDOM from terrestrial sources previously reported on (Opdal et al., 2023). According to the multiple regression analysis of the relationship between light attenuation and hydrographic predictors, a 200 μmol kg^{-1} drop in dissolved oxygen concentration was accompanied with a 0.054 m^{-1} increase in the light attenuation coefficient, K_{500} (Table 1). The concurrent increase in $a(\text{CDOM})_{500}$ (Fig. S5) suggests that the elevated K_{500} in the hypoxic and anoxic layers are due to locally produced CDOM rather than t-CDOM. We interfere this from the assumption that t-CDOM, which is brought to the sea with freshwater, should decrease, and not increase, when salinity increases such as in the hypoxic and anoxic layers of Haugsværfjorden.

The basin of Haugsværfjorden, i.e., the fjord volume situated below the sill depth of 25 m, contains water that has been trapped for some time. During such stagnant periods, the fjord basin receives sinking particulate organic matter (POM), which is degraded into DOM, and further processed by heterotrophic bacteria consuming dissolved oxygen and causing oxygen depletion. Previous studies report positive correlations between CDOM and the Apparent Oxygen Utilization (AOU, a proxy for microbial degradation and water mass aging) in the mesopelagic water masses of the open ocean (Catalá et al., 2015; Nelson and Siegel, 2013; Swan et al., 2009). In addition to CDOM production from microbial degradation consuming oxygen, anoxic coastal waters might experience further accumulation of CDOM under sulfidic conditions because of microbial degradation consuming sulfate as the oxidizing agent (Margolin et al., 2018). CDOM retained within sediments might also be released to overlying bottom waters under anoxic conditions (Kowalczuk et al., 2015; Loginova et al., 2016; Skoog et al., 1996). We find it likely that the elevated light attenuation in the oxygen-depleted waters in Haugsværfjorden partially arise from locally produced CDOM from microbial degradation of organic matter that sinks into the stagnant basin water. Below, we refer to this presumably local CDOM as l-CDOM.

When low-oxygen water (from mildly hypoxic to anoxic, dissolved oxygen <100 μmol kg^{-1}) was excluded from our regression analysis, only salinity and relative chlorophyll fluorescence remained significant predictors of light attenuation. This could suggest that the relationship between light attenuation and dissolved oxygen (and the associated l-CDOM) is only apparent in water masses with dissolved oxygen concentration below a certain threshold. An alternative explanation is that variations in t-CDOM and chlorophyll pigment concentration that occurred simultaneously with the reduction in dissolved oxygen in the upper 125 m of Masfjorden (dissolved oxygen decrease from ≈340 μmol kg^{-1} to ≈200 μmol kg^{-1}), and the upper 50 m of Haugsværfjorden (dissolved oxygen decrease from ≈350 μmol kg^{-1} to ≈100 μmol kg^{-1}), overshadowed associations between dissolved oxygen and l-CDOM.

The deeper basin water of Haugsværfjorden was anoxic and sulfidic during our cruises in 2020–2022. Data from August 2018, however, suggest that anoxia has not been a permanent feature of the basin as raw dissolved oxygen measurements from a CTD profile showed increasing oxygen from 85 m to 115 m depth (dissolved oxygen increased from 0.02 mL L^{-1} to 1.24 mL L^{-1}; see Fig. 3.2.4. D in Pitcher et al. (2021), which is equivalent to dissolved oxygen <1 μmol kg^{-1} to 54 μmol kg^{-1} respectively). Continued global warming is expected to cause reduced water renewal and enhanced deoxygenation, not only in Haugsværfjorden, but in many Norwegian fjords (Aksnes et al., 2019; Darelius, 2020; Johnsen et al., 2024). The shallower the sill depth, the larger the

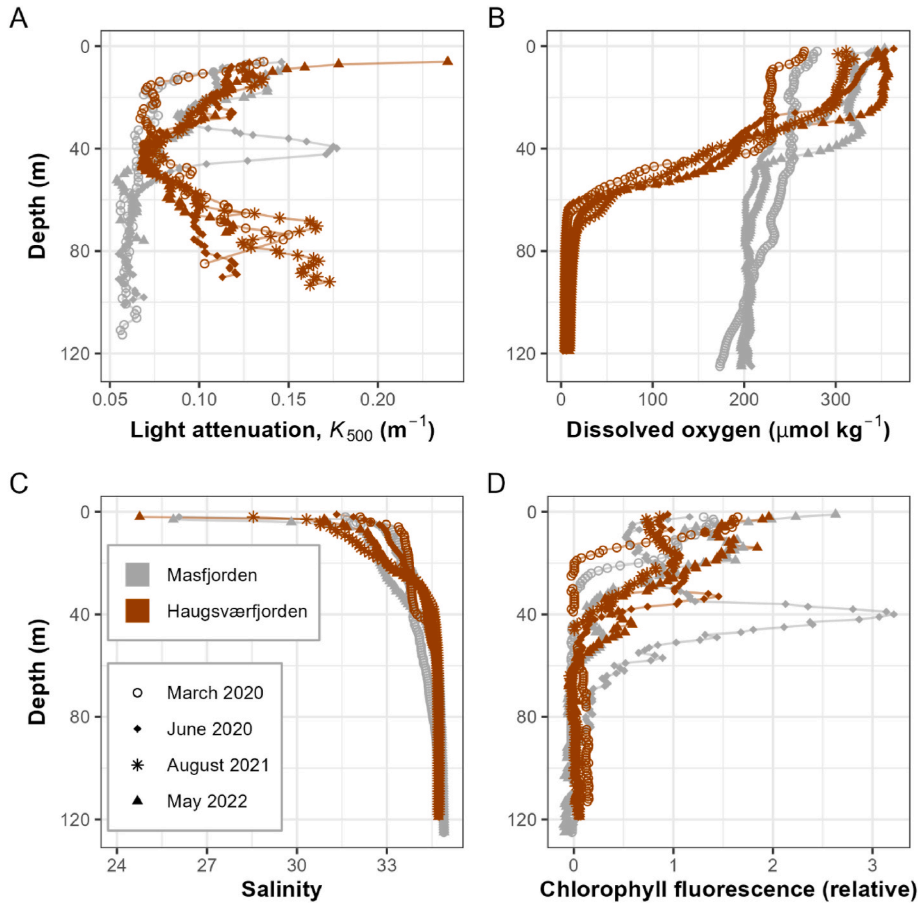

Fig. 3. Depth profiles (0–125 m) of (**A**) light attenuation coefficients of downwelling irradiance at 500 nm (K_{500}), (**B**) dissolved oxygen, (**C**) salinity and (**D**) relative chlorophyll fluorescence in Haugsværfjorden and Masfjorden. Sampling dates are listed in Table S1.

Table 1
Multiple linear regression results of light attenuation of downwelling irradiance (K_{500}) versus salinity, oxygen (µmol kg^{-1}) and relative chlorophyll fluorescence in Haugsværfjorden and Masfjorden (n = 435, $R^2_{adj.}$ = 0.66, p-value ≪ 0.001). SE is the standard error of the regression coefficient and β are the standardized regression coefficients that give an estimate of the relative contribution of the variation in each independent variable to the variation in the dependent variable (computed using the lm.beta R package (Behrendt, 2022)).

	Regression coefficient	SE	p-value	Standardized regression coefficient (β)
Intercept	1.218	0.0604		
Salinity	−0.0317	0.0017	**≪0.001**	−0.77
Oxygen (µmol kg^{-1})	−0.00027	0.00001	**≪0.001**	−0.97
Chlorophyll fluorescence (relative)	0.0276	0.0017	**≪0.001**	0.55

likelihood for deoxygenation (Aure and Stigebrandt, 1989) and associated l-CDOM darkening. Increased loads of t-CDOM brought to the sea by freshwater is also linked to global warming (Larsen et al., 2011; Opdal et al., 2023). While t-CDOM increases the light attenuation of upper water masses being affected by freshwater, l-CDOM increases the light attenuation at depths where deoxygenation occurs – resulting in a two-sided water darkening effect.

Such two-sided darkening has been associated with mesopelagic regime shifts in Norwegian fjords (Aksnes et al., 2009). Like in the ocean, deep fjords in Norway house large populations of mesopelagic fish and invertebrates that distribute vertically according to light and light penetration (Kaartvedt et al., 2019) and some species (e.g., lanternfishes) are likely tolerant of low oxygen levels (Olivar et al., 2017; Torres et al., 2012). Mesopelagic regime shifts in fjords have involved mass occurrences of the deep-water jellyfish, *Periphylla periphylla* (Fosså, 1992; Sørnes et al., 2007), which is a tactile feeder, apparently at the expense of mesopelagic fishes that are predominantly visual feeders (Aksnes et al., 2009; Eiane et al., 1999). Regime shifts involving visual constraints associated with darkening might be further exacerbated by low dissolved oxygen levels that can reduce light sensitivity and vision in marine organisms (McCormick et al., 2019, 2023).

In addition to previous reports of positive correlations between CDOM light absorption and AOU in oceanic areas (Catalá et al., 2015; Nelson and Siegel, 2013; Swan et al., 2009), elevated light attenuation of downwelling irradiance has been reported for hypoxic locations in the subtropical Atlantic and Pacific Oceans (Aksnes et al., 2017). Thus, an association between water darkening, l-CDOM production, and deoxygenation might be a general phenomenon that is common for mesopelagic waters in both coastal and oceanic areas. An important difference between coastal and oceanic areas, however, is that mesopelagic darkening in coastal areas might be magnified by the two-sided darkening effect. This is because coastal areas are more prone than oceanic areas to receive freshwater with elevated amounts of t-CDOM, as discussed in Opdal et al. (2023). Furthermore, the darkening associated with deoxygenation and l-CDOM in deep waters adds to the existing advice (e.g., Kampa, 1971; Kaartvedt et al., 2019) that light penetration of mesopelagic waters needs to be interfered from *in situ* light measurements in the mesopelagic rather than from extrapolation of attenuation coefficients derived for the upper water column.

CRediT authorship contribution statement

Martine Røysted Solås: Writing – review & editing, Writing – original draft, Visualization, Methodology, Investigation, Formal analysis, Data curation, Conceptualization. **Anne Gro Vea Salvanes:** Writing – review & editing, Supervision, Project administration, Investigation, Funding acquisition. **Dag L. Aksnes:** Writing – review & editing, Writing – original draft, Supervision, Methodology, Formal analysis, Conceptualization.

Declaration of competing interest

The authors declare that they have no known competing financial interests or personal relationships that could have appeared to influence the work reported in this paper.

Acknowledgements

We are grateful to The Research Council of Norway (HypOnFjordFish project number: 301077) for funding this research, to the crew members onboard the R.V. Kristine Bonnevie (Institute of Marine Research, IMR) for their contribution to collecting the data material, to Frank Midtøy (University of Bergen, UiB), Heikki Juhani Savolainen (UiB) and Arild Folkvord (UiB, IMR) for providing parts of the data material, and to Tom J. Langbehn (UiB) for sharing code relevant for some of the data import in this study.

Appendix A. Supplementary data

Supplementary data to this article can be found online at https://doi.org/10.1016/j.ecss.2024.108988.

GLOSSARY

Abbr.	Explanation	Unit
NCW	Norwegian coastal water.	
NCC	Norwegian coastal current.	
POM	Particulate organic matter.	
DOM	Dissolved organic matter. Organic material able to pass through a 0.2–0.4 μm filter (Nelson and Siegel, 2013).	
CDOM	Colored dissolved organic matter. DOM that absorbs solar radiation.	
t-CDOM	Here defined as CDOM of terrestrial origin.	
l-CDOM	Here defined as CDOM produced locally in marine waters by microbial degradation of POM.	
DCM	Deep chlorophyll maximum.	
K_{500}	Light attenuation coefficient from *in situ* measurements of downwelling irradiance at wavelength (λ) = 500 nm.	m^{-1}
$a(CDOM)_{500}$	CDOM light absorption at wavelength (λ) = 500 nm.	m^{-1}
Darkening	Water becomes darker because of increased light attenuation.	
AOU	Apparent oxygen utilization.	

Data availability

Data and code will be available in the Norwegian Marine Data Centre repository under an existing parent dataset (https://doi.org/10.21335/NMDC-92774636). Until then, data will be available on request.

References

Aksnes, D.L., 2015. Sverdrup critical depth and the role of water clarity in Norwegian Coastal Water. ICES J. Mar. Sci. 72, 2041–2050. https://doi.org/10.1093/icesjms/fsv029.

Aksnes, D.L., Aure, J., Johansen, P.-O., Johnsen, G.H., Salvanes, A.G.V., 2019. Multi-decadal warming of Atlantic water and associated decline of dissolved oxygen in a deep fjord. Estuar. Coast Shelf Sci. 228, 106392. https://doi.org/10.1016/j.ecss.2019.106392.

Aksnes, D.L., Aure, J., Kaartvedt, S., Magnesen, T., Richard, J., 1989. Significance of advection for the carrying capacities of fjord populations. Mar. Ecol. Prog. Ser. 50, 263–274. https://doi.org/10.3354/meps050263.

Aksnes, D.L., Dupont, N., Staby, A., Fiksen, Ø., Kaartvedt, S., Aure, J., 2009. Coastal water darkening and implications for mesopelagic regime shifts in Norwegian fjords. Mar. Ecol. Prog. Ser. 387, 39–49. https://doi.org/10.3354/meps08120.

Aksnes, D.L., Røstad, A., Kaartvedt, S., Martinez, U., Duarte, C.M., Irigoien, X., 2017. Light penetration structures the deep acoustic scattering layers in the global ocean. Sci. Adv. 3, e1602468. https://doi.org/10.1126/sciadv.1602468.

Aure, J., Stigebrandt, A., 1989. On the influence of topographic factors upon the oxygen consumption rate in sill basins of fjords. Estuar. Coast Shelf Sci. 28, 59–69. https://doi.org/10.1016/0272-7714(89)90041-3.

Behrendt, S., 2022. lm.beta: Add Standardized Regression Coefficients to Lm-Objects.

Capuzzo, E., Stephens, D., Silva, T., Barry, J., Forster, R.M., 2015. Decrease in water clarity of the southern and central North Sea during the 20th century. Global Change Biol. 21, 2206–2214. https://doi.org/10.1111/gcb.12854.

Catalá, T.S., Reche, I., Álvarez, M., Khatiwala, S., Guallart, E.F., Benítez-Barrios, V.M., Fuentes-Lema, A., Romera-Castillo, C., Nieto-Cid, M., Pelejero, C., Fraile-Nuez, E., Ortega-Retuerta, E., Marrasé, C., Álvarez-Salgado, X.A., 2015. Water mass age and aging driving chromophoric dissolved organic matter in the dark global ocean. Global Biogeochem. Cycles 29, 917–934. https://doi.org/10.1002/2014GB005048.

Darelius, E., 2020. On the effect of climate trends in coastal density on deep water renewal frequency in sill fjords—a statistical approach. Estuar. Coast Shelf Sci. 243, 106904. https://doi.org/10.1016/j.ecss.2020.106904.

Dupont, N., Aksnes, D.L., 2013. Centennial changes in water clarity of the Baltic Sea and the North Sea. Estuar. Coast Shelf Sci. 131, 282–289. https://doi.org/10.1016/j.ecss.2013.08.010.

Eiane, K., Aksnes, D.L., Bagøien, E., Kaartvedt, S., 1999. Fish or jellies-a question of visibility? Limnol. Oceanogr. 44, 1352–1357. https://doi.org/10.4319/lo.1999.44.5.1352.

Erlandsson, C.P., Stigebrandt, A., 2006. Increased utility of the Secchi disk to assess eutrophication in coastal waters with freshwater run-off. J. Mar. Syst. 60, 19–29. https://doi.org/10.1016/j.jmarsys.2005.12.001.

European Environment Agency, 2017. EEA Coastline for Analysis.

Fleming-Lehtinen, V., Laamanen, M., 2012. Long-term changes in Secchi depth and the role of phytoplankton in explaining light attenuation in the Baltic Sea. Estuar. Coast Shelf Sci. 102–103, 1–10. https://doi.org/10.1016/j.ecss.2012.02.015.

Fosså, J.H., 1992. Mass occurrence of periphylla periphylla (scyphozoa, coronatae) in a Norwegian fjord. Sarsia 77, 237–251. https://doi.org/10.1080/00364827.1992.10413509.

Frigstad, H., Andersen, G.S., Trannum, H.C., McGovern, M., Naustvoll, L.-J., Kaste, Ø., Deininger, A., Hjermann, D.Ø., 2023. Three decades of change in the Skagerrak coastal ecosystem, shaped by eutrophication and coastal darkening. Estuar. Coast Shelf Sci. 283, 108193. https://doi.org/10.1016/j.ecss.2022.108193.

Frigstad, H., Andersen, T., Hessen, D.O., Jeansson, E., Skogen, M., Naustvoll, L.-J., Miles, M.W., Johannessen, T., Bellerby, R.G.J., 2013. Long-term trends in carbon, nutrients and stoichiometry in Norwegian coastal waters: evidence of a regime shift. Prog. Oceanogr. 111, 113–124. https://doi.org/10.1016/j.pocean.2013.01.006.

GEBCO Compilation Group, 2023. GEBCO 2023 grid. https://doi.org/10.5285/f98b053b-0cbc-6c23-e053-6c86abc0af7b.

Giske, J., Aksnes, D.L., Baliño, B.M., Kaartvedt, S., Lie, U., Nordeide, J.T., Salvanes, A.G.V., Wakili, S.M., Aadnesen, A., 1990. Vertical distribution and trophic interactions of zooplankton and fish in Masfjorden, Norway. Sarsia 75, 65–81. https://doi.org/10.1080/00364827.1990.10413442.

Gjøsæter, H., Kawaguchi, K., 1980. A Review of the World Resources of Mesopelagic Fish. Food Agric. Organ. U. N, pp. 1–160.

Højerslev, N.K., Holt, N., Aarup, T., 1996. Optical measurements in the North Sea-Baltic Sea transition zone. I. On the origin of the deep water in the Kattegat. Continent. Shelf Res. 16, 1329–1342. https://doi.org/10.1016/0278-4343(95)00075-5.
Irigoien, X., Klevjer, T.A., Røstad, A., Martinez, U., Boyra, G., Acuña, J.L., Bode, A., Echevarria, F., Gonzalez-Gordillo, J.I., Hernandez-Leon, S., Agusti, S., Aksnes, D.L., Duarte, C.M., Kaartvedt, S., 2014. Large mesopelagic fishes biomass and trophic efficiency in the open ocean. Nat. Commun. 5, 3271. https://doi.org/10.1038/ncomms4271.
Johnsen, I.A., Loeng, H., Myksvoll, M.S., 2024. Coastal alterations influence deep water renewal in Norwegian sill fjords. Estuar. Coast Shelf Sci. 297, 108604. https://doi.org/10.1016/j.ecss.2023.108604.
Kaartvedt, S., Langbehn, T.J., Aksnes, D.L., 2019. Enlightening the ocean's twilight zone. ICES J. Mar. Sci. 76, 803–812. https://doi.org/10.1093/icesjms/fsz010.
Kahru, M., Bittig, H., Elmgren, R., Fleming, V., Lee, Z., Rehder, G., 2022. Baltic Sea transparency from ships and satellites: centennial trends. Mar. Ecol. Prog. Ser. 697, 1–13. https://doi.org/10.3354/meps14151.
Kampa, E.M., 1971. Photoenvironment and sonic scattering. In: Proceedings of an International Symposium on Biological Sound Scattering in the Ocean Maury Center for Ocean Science. U.S. Government Printing Office, Washington, DC, pp. 51–59.
Kowalczuk, P., Sagan, S., Zabłocka, M., Borzycka, K., 2015. Mixing anomaly in deoxygenated Baltic Sea deeps indicates benthic flux and microbial transformation of chromophoric and fluorescent dissolved organic matter. Estuar. Coast Shelf Sci. 163, 206–217. https://doi.org/10.1016/j.ecss.2015.06.027.
Larsen, S., Andersen, T., Hessen, D.O., 2011. Climate change predicted to cause severe increase of organic carbon in lakes. Global Change Biol. 17, 1186–1192. https://doi.org/10.1111/j.1365-2486.2010.02257.x.
Loginova, A.N., Thomsen, S., Engel, A., 2016. Chromophoric and fluorescent dissolved organic matter in and above the oxygen minimum zone off Peru. J. Geophys. Res. Oceans 121, 7973–7990. https://doi.org/10.1002/2016JC011906.
Margolin, A.R., Gonnelli, M., Hansell, D.A., Santinelli, C., 2018. Black Sea dissolved organic matter dynamics: insights from optical analyses. Limnol. Oceanogr. 63, 1425–1443. https://doi.org/10.1002/lno.10791.
McCormick, L.R., Gangrade, S., Garwood, J.C., Oesch, N.W., Levin, L.A., 2023. Oxygen and irradiance constraints on visual habitat in a changing ocean: the luminoxyscape. Limnol. Oceanogr. Lett. 220–228. https://doi.org/10.1002/lol2.10296.
McCormick, L.R., Levin, L.A., Oesch, N.W., 2019. Vision is highly sensitive to oxygen availability in marine invertebrate larvae. J. Exp. Biol. 222, jeb200899. https://doi.org/10.1242/jeb.200899.
Nelson, N.B., Siegel, D.A., 2013. The global distribution and dynamics of chromophoric dissolved organic matter. Ann. Rev. Mar. Sci 5, 447–476. https://doi.org/10.1146/annurev-marine-120710-100751.
Olivar, M.P., Hulley, P.A., Castellón, A., Emelianov, M., López, C., Tuset, V.M., Contreras, T., Molí, B., 2017. Mesopelagic fishes across the tropical and equatorial Atlantic: biogeographical and vertical patterns. Prog. Oceanogr. 151, 116–137. https://doi.org/10.1016/j.pocean.2016.12.001.
Opdal, A.F., Andersen, T., Hessen, D.O., Lindemann, C., Aksnes, D.L., 2023. Tracking freshwater browning and coastal water darkening from boreal forests to the Arctic Ocean. Limnol. Oceanogr. Lett. 8, 10320. https://doi.org/10.1002/lol2.10320 lol2.
Opdal, A.F., Lindemann, C., Aksnes, D.L., 2019. Centennial decline in North Sea water clarity causes strong delay in phytoplankton bloom timing. Global Change Biol. 25, 3946–3953. https://doi.org/10.1111/gcb.14810.
Opdal, A.F., Lindemann, C., Andersen, T., Hessen, D.O., Fiksen, Ø., Aksnes, D.L., 2024. Land use change and coastal water darkening drive synchronous dynamics in phytoplankton and fish phenology on centennial timescales. Global Change Biol. 30, e17308. https://doi.org/10.1111/gcb.17308.
Pitcher, G.C., Aguirre-Velarde, A., Breitburg, D., Cardich, J., Carstensen, J., Conley, D.J., Dewitte, B., Engel, A., Espinoza-Morriberón, D., Flores, G., Garçon, V., Graco, M., Grégoire, M., Gutiérrez, D., Hernandez-Ayon, J.M., Huang, H.-H.M., Isensee, K., Jacinto, M.E., Levin, L., Lorenzo, A., Machu, E., Merma, L., Montes, I., Naqvi, S.W.A., Paulmier, A., Roman, M., Rose, K., Hood, R., Rabalais, N.N., Salvanes, A.G.V., Salvatteci, R., Sánchez, S., Sifeddine, A., Tall, A.W., Plas, A.K. van der, Yasuhara, M., Zhang, J., Zhu, Z., 2021. System controls of coastal and open ocean oxygen depletion. Prog. Oceanogr. 197, 102613. https://doi.org/10.1016/j.pocean.2021.102613.
R Core Team, 2022. R: A Language and Environment for Statistical Computing.
Sætre, R., 2007. The Norwegian Coastal Current: Oceanography and Climate. Tapir Academic Press.
Sandén, P., Håkansson, B., 1996. Long-term trends in secchi depth in the Baltic Sea. Limnol. Oceanogr. 41, 346–351. https://doi.org/10.4319/lo.1996.41.2.0346.
Skoog, A., Hall, P.O.J., Hulth, S., Paxéus, N., Van Der Loeff, M.R., Westerlund, S., 1996. Early diagenetic production and sediment-water exchange of fluorescent dissolved organic matter in the coastal environment. Geochem. Cosmochim. Acta 60, 3619–3629. https://doi.org/10.1016/0016-7037(96)83275-3.
Sørnes, T.A., Aksnes, D.L., Bamstedt, U., Youngbluth, M.J., 2007. Causes for mass occurrences of the jellyfish Periphylla periphylla: a hypothesis that involves optically conditioned retention. J. Plankton Res. 29, 157–167. https://doi.org/10.1093/plankt/fbm003.
Stedmon, C.A., Markager, S., 2003. Behaviour of the optical properties of coloured dissolved organic matter under conservative mixing. Estuar. Coast Shelf Sci. 57, 973–979. https://doi.org/10.1016/S0272-7714(03)00003-9.
Stigebrandt, A., Andersson, A., 2020. The eutrophication of the Baltic Sea has been boosted and perpetuated by a major internal phosphorus source. Front. Mar. Sci. 7, 572994. https://doi.org/10.3389/fmars.2020.572994.
Swan, C.M., Siegel, D.A., Nelson, N.B., Carlson, C.A., Nasir, E., 2009. Biogeochemical and hydrographic controls on chromophoric dissolved organic matter distribution in the Pacific Ocean. Deep-Sea Res. Part A Oceanogr. Res. Pap. 56, 2175–2192. https://doi.org/10.1016/j.dsr.2009.09.002.
Torres, J.J., Grigsby, M.D., Clarke, M.E., 2012. Aerobic and anaerobic metabolism in oxygen minimum layer fishes: the role of alcohol dehydrogenase. J. Exp. Biol. 215, 1905–1914. https://doi.org/10.1242/jeb.060236.
Turner, J.R., White, E.M., Collins, M.A., Partridge, J.C., Douglas, R.H., 2009. Vision in lanternfish (Myctophidae): adaptations for viewing bioluminescence in the deep-sea. Deep-Sea Res. Part A Oceanogr. Res. Pap. 56, 1003–1017. https://doi.org/10.1016/j.dsr.2009.01.007.
Warrant, E.J., Locket, A.N., 2004. Vision in the deep sea. Biol. Rev. 79, 671–712. https://doi.org/10.1017/S1464793103006420.
Wickham, H., Averick, M., Bryan, J., Chang, W., McGowan, L.D., François, R., Grolemund, G., Hayes, A., Henry, L., Hester, J., Kuhn, M., Pedersen, T.L., Miller, E., Bache, S.M., Müller, K., Ooms, J., Robinson, D., Seidel, D.P., Spinu, V., Takahashi, K., Vaughan, D., Wilke, C., Woo, K., Yutani, H., 2019. Welcome to the tidyverse. J. Open Source Softw. 4, 1686. https://doi.org/10.21105/joss.01686.
Wihtakari, M., 2024. ggOceanMaps: Plot Data on Oceanographic Maps Using "ggplot2.".
Wilson, R.J., Heath, M.R., 2019. Increasing turbidity in the North Sea during the 20th century due to changing wave climate. Ocean Sci. 15, 1615–1625. https://doi.org/10.5194/os-15-1615-2019.